Colloids and Surfaces A: Physicochemical and Engineering Aspects 682 (2024) 132983

Contents lists available at ScienceDirect

Colloids and Surfaces A: Physicochemical and Engineering Aspects

journal homepage: www.elsevier.com/locate/colsurfa

Colloidal properties of polymer amended Cyprus bentonite for water-based drilling fluid applications

Youstina Ramsis [a], Elias Gravanis [b], Ernestos Sarris [a,c,*]

[a] Department of Engineering, Oil and Gas Program, University of Nicosia, Nicosia CY-2409, Cyprus
[b] Department of Civil Engineering and Geomatics, Cyprus University of Technology, Limassol CY-3036, Cyprus
[c] School of Geology, Department of Minerology-Petrology-Economic Geology, Aristotle University of Thessaloniki (AuTH), Greece

GRAPHICAL ABSTRACT

The cationic bridging adsorption effect leads to electrostatic attractions developed between the carboxylate anions of xanthan gum polymer and the interlayer space cations of Polycanthos bentonite. Then bentonite becomes a polymer-amended material resulting in the colloidal composite structure. The desired colloidal properties for water-based drilling fluid applications are obtained when the shear stress reaches 15.31 Pa or higher at 600 rpm, according to API specifications.

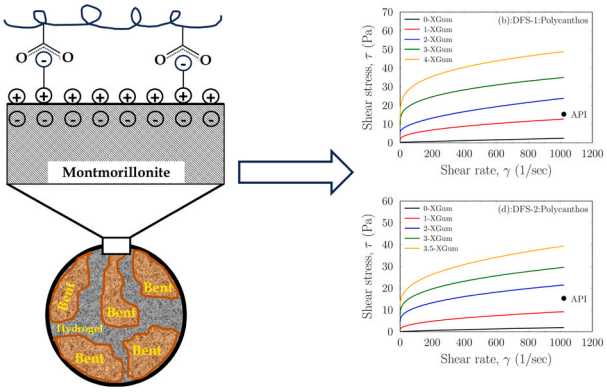

ARTICLE INFO

Keywords:
Soda-ash activation methods
Drilling fluid systems
K^+-bentonite
Xanthan gum polymer amendment
Circular economy
Sustainable development

ABSTRACT

In this work, we investigate the capability of a waste bentonite from the Polycanthos quarry in Cyprus, as a low-density solid additive to create colloids that are used in water-based drilling fluid systems (WBF) in drilling operations. Repurposing waste bentonite aligns with environmental sustainability and when properly processed can serve as a cost-effective solution to achieve the desired colloidal properties for WBF. Samples were obtained from waste stockpiles and were mechanically processed to a size < 63 μm. The material was activated with soda ash via three different methods investigating optimum soda ash percentage and curing time. Standard tests were performed for the rheological behavior and filtration properties and the results indicated that the quality of the activated clay dispersions improved slightly but the desired colloidal properties were not obtained. This can be attributed to the K^+-rich clay and non-clay impurities that are inherent in the material so further amendment with xanthan gum polymer was conducted, at various concentrations. Results of this work show that with minor polymer addition, the material under investigation reaches the desired colloidal properties and qualifies

* Corresponding author at: Department of Engineering, Oil and Gas Program, University of Nicosia, Nicosia CY-2409, Cyprus.
E-mail address: sarris.e@unic.ac.cy (E. Sarris).

https://doi.org/10.1016/j.colsurfa.2023.132983
Received 7 October 2023; Received in revised form 26 November 2023; Accepted 11 December 2023
Available online 14 December 2023

according to API standards for WBF. Exploiting local waste clay material in WBF application leads to the development and sustainability of local resources thus contributing to the circular economy principle.

1. Introduction

The exponential increase in energy demand but at the same time the protection of the environment from greenhouse gas emissions has become a global concern and has led hydrocarbon operators to turn their focus to the recovery of environmentally friendly resources like natural gas but also to renewable energy sources like geothermal energy. The European Union has focused on sustainability, through a series of reforms, with the overarching aim that by 2030 renewable energy sources will replace the conventional resources that are produced from coal and petroleum, thus contributing to a significant reduction of greenhouse gas emissions (mainly CO_2 by at least 50% as compared to 1990 levels) in the atmosphere. Another aim is that by 2050 the circular economy should become "an applied model" for large and advanced economies adopting the perception of '*waste as a resource*'. That aim in March 2020, set the basis for the Green Deal policy of the European Commission. The key factor for applying the Green Deal policy is the threefold reuse, recycling, and renovation rule which is thought to satisfy the future demand for raw materials [1–6].

Recently, in the Eastern Mediterranean significant discoveries of offshore gas reservoirs have been discovered summing up to 12 trillion cubic feet (TCF) to date, while exploration activities are continuing. The current exploratory gas wells but also later for gas production wells, have increased the drilling operations in Cyprus and hence the demand for raw materials used in drilling fluid systems. As in any other EU country, strict environmental regulations and legislations exist that dictate the use of water-based drilling fluid systems (WBF) in drilling operations. While the exploration phase is in the early stages of operations, drilling companies attempt to reduce costs by avoiding imports and prefer to use domestic raw materials for the preparation of their drilling fluid systems. This realization has led to the increase of low-density solids (bentonite) demand in Cyprus. It is also worth noting that the drilling activity is not limited to the economic exclusive zone (EEZ) of Cyprus but extends to other neighbouring countries like Israel, Lebanon, and Egypt. As such, it is not surprising that mining companies are trying to adapt to this new industrial demand. However, before using bentonite in drilling fluid systems, its performance must be investigated in the context of rheological and filtration properties to meet the API standards [7–10].

Bentonite is a well-known material for its excellent colloidal properties in aqueous systems. These excellent colloidal characteristics are attributed to montmorillonite (Mt) clay mineral when is higher than 80% and is Na^+-rich. Industrially, sodium montmorillonite satisfies the requirement for water-based drilling fluid applications, based on API specifications, but is inappropriate when the predominant species in the interlayer space of montmorillonite is not Na^+. However, Ca^{2+}-rich or even Mg^{2+}-rich bentonite can still be used for the so-called "*pump and dump*", that is, drill the upper well section with water-based fluid and then release the cuttings and drilling fluid at sea. Controversially, K^+ is the only alkali metal that does not hydrate rendering the creation of colloids a major challenge [11–16].

From the mining industry's standpoint of view, non-sodium material is required to be chemically treated, a process known as *"activation" or "cation exchange reaction"*, to become Na^+ rich, hence commercial. Numerous authors have proposed multiple methods with various chemical compounds to activate bentonite clay under different conditions for water-based drilling fluids. The widely applied method proposed by many authors and adopted by the mining industry is the activation with Na_2CO_3 exclusively under dry, wet, or thermal conditions. When activated bentonite does not create colloids, polymer additives are used to enhance its viscous performance. Polymers include within their structure ionizable functional groups and when exposed to water they ionize into cations or anions presenting hydrophilic behaviour suitable for fluid-loss inhibitors and as viscosifiers. These are adsorbed in the interlayer space in montmorillonite and polymer-amended bentonite is obtained. Among all modifications, cationic, anionic, or neutral type, the anionic is the most effective. Multiple types of bonds and interactions are created (cationic bridging adsorption; hydrogen bonding and electrostatic attraction between edge positive charges in montmorillonite and the anionic groups of polymers) which do not predominate with others. As a result, more stable colloids are created. [17–31].

In this work, low-quality waste bentonite was provided from Polycanthos quarry that belongs to Hellenic Mining Company Ltd and activated with Na_2CO_3 under dry, wet, and thermal conditions to create the desired colloidal properties. As a second investigation, we amended the bentonite with xanthan gum polymer. For this reason, we have prepared two drilling fluid systems. The first one contains thermally Na_2CO_3-activated bentonite, xanthan gum, barite, and NaOH suitable for drilling an upper well section. The second one contains also thermally Na_2CO_3-activated bentonite (in less quantity), xanthan gum, barite, NaOH, and KOH suitable for drilling the pay zone. The evaluation of the effect of Na_2CO_3 and the effect of the xanthan gum as a functional additive are investigated macroscopically through rheological parameters and filtration properties specified by API guidelines. API standards for filtration properties are satisfied when fluid losses are less than 15 mL while colloidal properties are related to rheological parameters and specifically the viscometer dial reading for shear stress measurement at 600 rpm is minimum equal to 15.31 Pa. For comparisons, we have used commercial bentonite to prepare both drilling fluid systems as a reference [8,9]. The novelty of the work lies in the environmental sustainability and cost-effective value of the waste bentonite, which can achieve the desired colloidal properties for WBF after the polymer addition. Amending or enhancing local clays to be used as additives in drilling fluids, leads to the development and sustainability of local resources. The colloidal aspects are key to the experiments and discussion of the manuscript.

This contribution is organized as follows: in Section 2 we describe the geology of the formation and any relevant information about Polycanthos quarry is stated. Section 3 describes the materials and methods used for the activation methodologies and the experimental setup description. Section 4 presents the results obtained from this work and their discussion. Furthermore, the outcomes from the experiments of the activated material and the polymer amendment in complete drilling fluid systems are analyzed. Finally, Section 5 outlines the main findings of this work.

2. Geological description

In Cyprus, Troodos is an ophiolite complex that is dated at about 93 Ma. Troodos has many clay deposits because of the alteration of the upper Cretaceous basic pyroclastic rocks, overlaying upper pillow lavas of the ophiolitic complex. The magmatic complex of Troodos is overlain by pelagic sediments of the Kanaviou and the Para-pedi formations, which include radiolarian shales, manganese shales, umbers, and mudstones of the Campanian-Maastrichtian age. These formations are then followed by clay-bentonite beds of similar age. These bentonites are overlayed by a Cretaceous-Triassic melange. The resulting smectites are stratified, well-compacted bodies with a thickness ranging from a few to tens of meters depending on stratigraphy. They have been affected by three fault systems having EW, NS, and NE-SW directions. In places, they have thin layers (up to 1 cm thick) of opal-CT-rich material. Their

contact with the overlying reef limestones and the underlying pillow lavas is discontinuous. Such bodies, however, present significant amounts and of economic importance clay-bentonite material, attractive for commercial exploitation. Fig. 1 shows the geological cross-section of Polycanthos quarry which belongs to Hellenic Mining Company Ltd and is one of the cases that contains significant amounts of raw clay material, however, the resulting smectite is metal-rich montmorillonite which limits its commercial exploitation for various usages.

As can be seen from Fig. 1, there are four types of bentonite beds from top to bottom of the deposit, and these are green-grey bentonite, brown-reddish bentonite, reddish-ginger bentonite, and grey bentonite. In some places, umbers exist, which are black bentonite horizons, i.e., Mn-rich horizons. The mineral assemblage of Polycanthos bentonite quarry consists of smectite at 40–60% as the major mineral but also contains quartz at 10–30% and opal-CT in large quantities. Some minor quantities of other minerals are also present, such as illite/mica, kaolinite, palygorskite, clinoptilolite (HEU-type zeolite), plagioclase, calcite, dolomite, siderite, and finally todorokite in very minor quantities. To conclude, the Polycanthos deposit contains traces of minerals like chlorite, K-feldspar, apatite, goethite, hematite, ilmenite, and dioxide of titanium (TiO_2) and halite. The analysis for the compositional synthesis of the deposit was sampled from various locations chosen appropriately to be representative of the material. It was shown that smectite is composed of multiple oxides with SiO_2 being the main crystal in the smectitic structure and varies between 59–68%. The second highest content oxide is Al_2O_3 which varies between 15–24%.

Furthermore, traces of other oxides exist in the following concentrations: 10 ppm to 17% w/w of Fe_2O_3, 3.4 to 4.3% w/w of MgO, 5 ppm to 2.5% w/w of Na_2O, 2 ppm to 1% w/w CaO, and 0 to 3% w/w K_2O. All samples examined include moderate content of potassium ions and high-octahedral iron and are rich in Fe^{3+} montmorillonite. All these data represent all bentonite samples from the Polycanthos deposit [7].

3. Materials and methods

3.1. Materials used in the experiments

Commercial bentonite was acquired from Milos Island in Greece branded as Zenith® provided by IMERY'S minerals. The Na_2CO_3 agent, with concentration $\geq$ 98% w/w and $\leq$ 100% w/w, was acquired from Solvay Chemicals International in Brussels-Belgium, and the polymer xanthan gum branded "*free*" is acquired from Doves Farm Foods in the UK. Barite was acquired from Kemira-KemDrill LTD in Portugal.

3.2. Materials and drilling fluid systems preparation

During a drilling operation, the well may be divided into two sections, "upper" and "lower" well section. The reason for dividing the well into two sections is to avoid formation damage when the pay zone is reached and penetrated. The main idea behind the well section separation is to limit filtrate losses as best as possible in the lower well section. The first drilling fluid system (DFS1) is prepared to simulate the requirements of the upper well section while the "drill-in" fluid system (DFS2) satisfies the requirements of the lower well section when the pay zone is reached. For comparisons, we have used commercial bentonite from Milos Island in Greece branded as Zenith®, and thermally activated Bentonite from Polycanthos quarry in Cyprus. Furthermore, Polycanthos bentonite was amended with xanthan gum through these two drilling fluid systems. The final volume of each system prepared is 350 mL which is equivalent to one barrel. The tests were conducted at standard conditions.

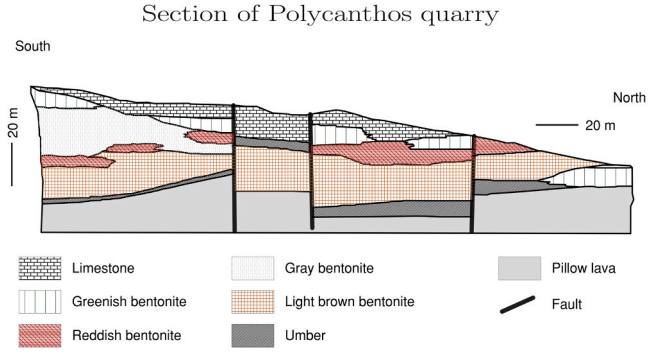

Fig. 1. Geologic cross-section of Polycanthos deposit with the various bentonite horizons.

For the purposes of this analysis, four DFS-1A were prepared with commercial bentonite and other additives to form the final mixture. Each additive is mixed in distilled water and blended in a Fann mixer for 5 min. When all additives are included, the final mixture has a final volume of 350 mL which is equivalent to one barrel of DFS-1A. It should be noted that the Na_2CO_3 compound is not mixed with the commercial bentonite because it is already activated. Furthermore, it does not require the addition of NaOH because it already presents the desired colloidal properties [11,12,37]. The same procedure was repeated for the drilling fluid system with thermally activated Polycanthos bentonite (DFS-1B) with 1.5% w/v Na_2CO_3 at 50 ^{0}C and agitating for 16 h. These conditions were found to be optimal after experimental investigation of the activation methods' performance. In total, 9 different drilling fluid systems were prepared. Four with commercial bentonite (DFS-1A) while five with thermally activated Polycanthos bentonite (DFS-1B). Each mixture is tested at standard conditions to determine the rheological parameters and filtration properties based on the API guidelines. Tables 1 & 2 present the additives and their masses added for each DFS, with commercial and Polycanthos bentonite respectively.

The second group of tests (DFS-2) were for the case of the lower well section. The procedure followed for this case was like the one described for the upper well section. The DFS mixtures were prepared for both, with thermally activated bentonite from Polycanthos and with commercial. As in the previous case, 9 different drilling fluid systems were synthesized. Four with commercial bentonite (DFS-2A) and five with Polycanthos bentonite (DFS-2B). Tables 3 & 4 present the additives and their masses added for each DFS, with commercial and Polycanthos bentonite respectively. Finally, the tests were conducted at standard conditions.

3.3. Description of the activation methods

The following paragraph describes the procedure that was used for activating the raw bentonite from the Polycanthos deposit under dry conditions. Polycanthos waste bentonite was downsized with a small lab-scale disc mill to less than 1 mm and then it was sieved to obtain a grain diameter that was less than 63 μm. Then, 16 bentonite clay samples, all with grain size diameter < 63 μm and with a weight of 22.5 gr, each, were placed in molds. Four different concentrations of Na_2CO_3 (1.5, 3, 6, 12% w/w) were added to the molds and then kneaded until the soda ash mass until complete homogenization with the raw bentonite material. To replicate industrial field conditions of dry activation, all samples were placed in the oven at a temperature of 35 ^{0}C which is the mean temperature in Cyprus, simulating curing under the

Table 1
Drilling fluid system with commercial bentonite (DFS-1A).

DFS-1A	Mass (lb)
Distilled Water	***{336.62 – 335.95–335.62 – 335.28}***
Bentonite (viscosifier, LD solid)	22.5
X.gum (viscosity enhancement)	***{0 – 1 – 1.5 – 2}***
Barite (density control, HD solid)	1
Final density (ppg)	***{8.57 – 8.58 – 8.586 – 8.59}***

Table 2
Drilling fluid system with Polycanthos activated bentonite (DFS-1B).

DFS-1B	Mass (lb)
Distilled Water	***{334.08 – 333.41–332.74 – 332.08 – 331.41}***
Bentonite (viscosifier, LD solid)	22.5
Na_2CO_3 (activator)	5.25
NaOH (pH controller)	1
X.gum (viscosity enhancement)	***{0 – 1 – 2 – 3 – 4}***
Barite (density control, HD solid)	1
Final density (ppg)	***{8.66 – 8.67 – 8.678 – 8.686 – 8.694}***

Table 3
Drilling fluid system with commercial bentonite (DFS-2A).

DFS-2A	Mass (lb)
Distilled Water	***{342.83 – 342.17–341.83 – 341.5}***
Bentonite (viscosifier, LD solid)	6
NaOH (pH controller)	1
KOH (shale stabilizer)	5
X.gum (viscosity enhancement)	***{0 – 1 – 1.5 – 2}***
Barite (density control, HD solid)	5
Final density (ppg)	***{8.567 – 8.575 – 8.579 – 8.583}***

Table 4
Drilling fluid system with Polycanthos activated bentonite (DFS-2B).

DFS-2B	Mass (lb)
Distilled Water	***{340.77 – 340.1 – 339.43 – 338.77 – 338.43}***
Bentonite (viscosifier, LD solid)	6
Na_2CO_3 (activator)	5.25
NaOH (pH controller)	1
KOH (shale stabilizer)	5
X.gum (viscosity enhancement)	***{0 – 1 – 2 – 3 – 3.5}***
Barite (density control, HD solid)	5
Final density (ppg)	***{8.64 – 8.651 – 8.659 – 8.667 – 8.671}***

sun. Finally, the mixed material in the molds was kneaded daily throughout the duration of the curing process for better mixing and drying of the bentonite. The kneaded samples were left to cure for 7, 14, 21, and 30 days respectively. Fig. 2a presents the dry-activated sample.

The second activation method was performed under wet conditions. With this activation method, a solution was prepared by adding a calculated quantity of Na_2CO_3 corresponding to 1.5%, 3%, 6%, and 12% w/v respectively in distilled water and was left to mix in a Fann mixer for 5 mins. Then, 22.5 gr mechanically processed bentonite was added, ensuring a final volume 350 mL of the dispersion, was mixed for another 10 mins. The produced dispersions were placed in glass jars and left to cure as in the dry activation method, for 7, 14, 21, and 30 days.

Finally, we have used a thermal activation methodology for activating the bentonite. With this novel method, two different temperatures were examined at 50 ^{0}C and 80 ^{0}C. The prepared dispersion, which was identical to the wet activation mixture, was left to agitate for 16 and 32 h respectively to achieve optimum mixing and with the different temperature levels to increase the rate of cation exchange reaction and hence the activation performance. 48 dispersion samples in total were obtained from the activation methods to evaluate if the desired colloidal properties have been obtained and if the filtration properties could satisfy API specifications. Fig. 2b presents the wet and thermally activated samples.

3.4. Method for the colloidal properties' evaluation - Rheology

A complete rheological characterization was conducted on each bentonite dispersion produced from each activation method and on all the drilling fluid system mixtures. Rheological tests were conducted with the help of a Couette-type rheometer by Fann (model-35A) which has six gears (3, 6, 100, 200, 300, and 600 rpm) assisting in the determination of the rheological model but also to obtain the two major rheological parameters, plastic viscosity (PV) and yield point (YP). The latter is obtained by getting the reading from the dial when the rotational speed is equal to ω = 300 rpm and ω = 600 rpm. These parameters are related to the industrially accepted Bingham-Plastic rheological model through [32]:

$$\tau = \tau_{Yield} + \mu_P \dot{\gamma} \tag{1}$$

where τ is the shear stress (dynes/cm^2 = 4.79 lbs/100 ft^2), τ_{Yield} is the yield stress (dynes/cm^2 = 4.79 lbs/100 ft^2), μ_P is the plastic viscosity (dyne x sec/cm^2) and $\dot{y}$ is the shear rate (sec^{-1}). The plastic viscosity μ_P is obtained from the expression:

$$\mu_P = \mathrm{PV}^{Bingham} = \left(\omega_{600} - \omega_{300}\right) \tag{2}$$

where ω_{600} and ω_{300} is the rotational speed at 600 and 300 rpm, respectively. The yield stress is related to the yield point through:

$$\tau_Y = \mathrm{YP}^{Bingham} = \left(\omega_{300} - \mathrm{PV}^{Bingham}\right) \tag{3}$$

The acceptance of this rheological model from the industry has powered many researchers to investigate the validity of the Bingham plastic rheological model and have proven that is only valid for special types of drilling fluids, and it may yield inadequate results for lower rotational speeds ω = [3, 6, 100, 200] rpm which are the remaining from the complete shear rate range for most drilling dispersions [33,34]. This inconsistency is combated with the Herschel-Bulkley or the yield power-law rheological model given by:

$$\tau = \tau_Y + K(\dot{\gamma})^n \tag{4}$$

where K is the consistency index (dyne x sec^n/cm^2), and n is the power-law index (-). However, the determination of the yield stress, the

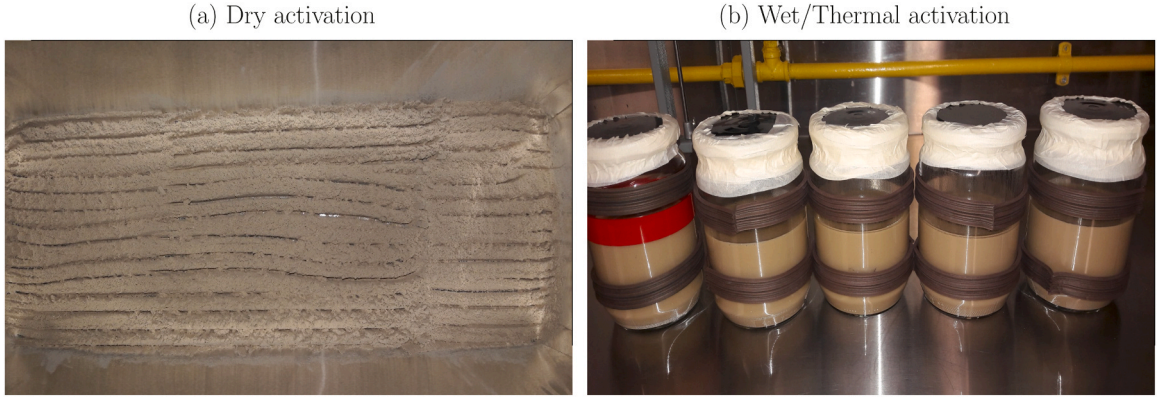

Fig. 2. Bentonite preparation for (a) dry and (b) wet/thermal activation methods.

consistency index, and the power-law index are not trivial as it involves the best fit of non-linear behavior in the low shear rates regime through a set of six points obtained from the Fann rheometer recognized as a non-linear optimization problem. To work around this minor difficulty, the Generalized Reduced Gradient (GRG) Method was used which is considered to be one of the most popular methods for solving nonlinear optimization problems [35].

The rheology of the drilling fluid is determined with the help of the Fann Couette viscometer to determine the rheological properties of the prepared drilling fluid system. Before testing starts, the Couette viscometer is assembled. The drilling fluid system is prepared and mixed thoroughly to ensure homogeneity before testing. Then the viscometer cup is filled to a designated line with the drilling fluid in such a way as to avoid introducing air bubbles. When the cup is in place the viscometer is operated at six operating speeds of {3, 6, 100, 200, 300, 600} rpm, and the dial reading is recorded after allowing rotation for a sufficient amount of time to stabilize the reading. The record is a deflection angle caused by the shearing of the fluid that depends strongly on the drilling fluid system under evaluation. When the data are obtained, the shear rate against the corresponding shear stress is plotted on the graph following the methodology of Section 3.4. From the determined rheological properties of the drilling fluid system, we obtain information for optimizing the proposed drilling fluid formulations.

3.5. Method for fluid losses evaluation – LPLT Filtration

The determination of the static filtration properties and the filter cake-building characteristics of newly proposed drilling fluids are fundamental to the drilling operation and well control. Experimentally, the filtration properties are the measure of separation and collection of filtrate fluid (in mL) from the dispersion and the build-up solids at the porous and permeable paper creating the filter cake (in mm). Theoretically, according to [36], one may consider that a certain volume of drilling fluid (solid-phase and fluid-phase mixed) is filtered through a permeable porous substrate. Assuming that (i) the cake stabilizes (becomes constant) and (ii) the applied pressure of the experiment is constant (boundary condition), then the volume of the filtrate is given by:

$$V_{filtrate} = \sqrt{\frac{2A^2.\kappa.P.n.t}{\mu(1-n)}} \tag{5}$$

where A is the cross-sectional area of the filter in mm^2, κ is the filter cake permeability, P is the applied pressure equal to 100 psi, n is a unit volume filtrate, t is time (30 mins), and μ is the viscosity of the drilling fluid system to be tested. Examining expression (5) it is observed that the filtrate volume is (i) analogous to the cross-sectional area of the permeable porous substrate, (ii) to the square root of time dictating that the deposition of cake is a self-similar phenomenon, (iii) to the square root of the ratio of permeability to the filtrate viscosity and (iv) to the square root of pressure. The remaining terms are constants. Some further factors affecting the fluid loss from the dispersion stem from Darcy's fluid flow (flow through the filter cake) depend on the quantity, type, and size of solid particles. Eq. (6) is important because it allows for the determination of the permeability under the assumption that the cake has stabilized, and the pressure gradient is stabilized.

$$\kappa = \frac{\left(V_{filtrate}\right)^2 \mu(1-n)}{2.A^2.P.n.t} \tag{6}$$

where κ (the permeability of the filter cake) has units of area (mm^2) or equivalent (mD) units.

The filtration properties of the proposed drilling fluids were determined through a Low Pressure and Low Temperature (LPLT) filter press by Fann which is built according to the API recommended practice guidelines. According to the procedure, a certain amount of drilling fluid system is added to the LPLT cell after inserting a mesh screen with filter paper on top. Then the cell is secured on the press apparatus and a constant pressure of 100 psi is applied via a CO_2 cartridge while, in parallel, time is recorded immediately after the pressure application. Due to the instant application of the pressure with the synchronous time recording, there is a small number of gases that exit from the cell a well-known phenomenon called "*spurt-loss*" until the cake stabilizes. It should be noted that no gases were observed during any of the tests and as such this phenomenon did not influence the outcomes of this research work in any way. After the end of the experiment, the filter cake thickness is measured in mm but also the filtrate is collected in (mL) after noting time at the first 7.5 min and then again at 30 min of the experiment duration. According to API regulations, the filtrate volume collected at 30 min must not exceed 15 mL, otherwise re-designing the fluids is necessary [32,36].

The static filtration is performed with the Fann Low Pressure-Low Temperature (LPLT) Filter Press which is a device used for measuring the filtration properties of drilling fluids. With this test, the fluid loss characteristics of the drilling fluid are determined under constant pressure conditions of 100 psi and for 30 mins. First, the LPLT filter press is assembled. Then, a representative volume of the prepared drilling fluid system is poured into the filter press cell. After applying pressure, the fluid phase is forced through the filter paper while the solid phase is accumulating on the filter paper in the cell. The pressure level of 100 psi, simulates the conditions the fluid would experience downhole. The fluid that passes through the filter paper is called the Filtrate and is collected in a graduated tube. The filtrate volume is recorded at 7.5 mins initially and then at 30 mins at the end of the experiment. The test results include the volume of filtrate that was lost in (mL) and the cake building thickness in (mm). This information helps to assess the effectiveness of the drilling fluid in terms of fluid loss control evaluating the filtration characteristics of the drilling fluid system.

4. Results and discussion

In this section, we present and evaluate the results from the experimental analysis that has been performed. The discussion is organized into the performance of the activation methods following the polymer amendment that has been proposed to enhance bentonite to reach API specifications.

4.1. Activations' performance: rheology

The first part of the analysis is concerned with the rheological characterization of the fluid dispersion after activation.

Fig. 3a to d presents the rheological curves of the dispersions for the different activation concentrations 1.5%, 3%, 6%, and 12% w/w respectively (denoted in the Figures with the letter A) after allowed to cure for 7, 14, 21, and 30 days with the dry activation method. Each curve represents a different curing time (denoted in the Figures with the letter C) and for completeness, the rheological results from a non-activated dispersion (raw) were included (denoted with N-A in the Figures).

By examining Fig. 3 it is observed that for most rheological curves, shear rates corresponding to θ_{300} and higher, present linear behavior but for lower shear rates (e.g., between θ_3 ⁻ θ_{200}) the curves are nonlinear. The most appropriate model to describe this rheological behavior is the Herschel-Bulkley model. Results corresponding to various percentages of soda ash suggest that the optimum curing time is around *14 days* with a *soda ash concentration of 3% w/w*. Longer curing times (e.g., 21 and 30 days) cause the rheological curve to reduce its plastic viscosity and yield stress, deeming the dispersion inadequate. The result for the activation percentage of 12% w/w does not represent any significant improvement but also the excess of soda ash appears to have a negative effect on the rheological parameters (plastic viscosity and yield stress) produced by the dispersion. On the other hand, the activation percentage of 1.5% w/w requires more curing time – 21 days suggesting that the activation

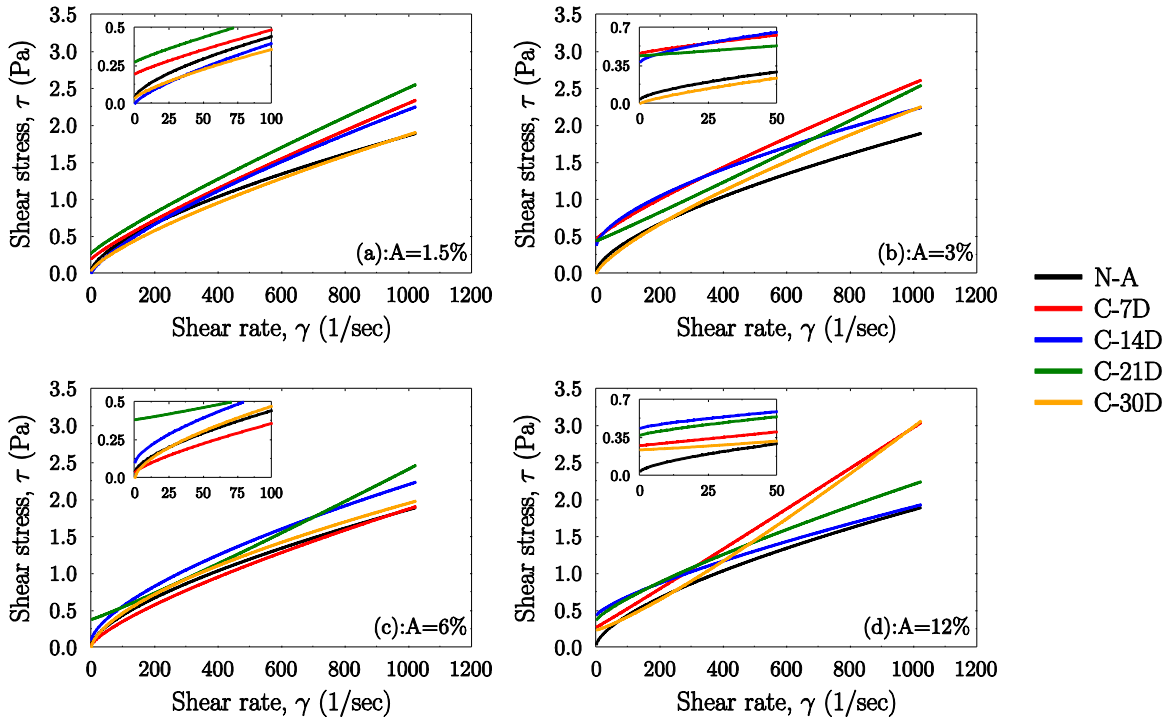

Fig. 3. Rheological curves for various activation concentrations: (a) 1.5%, (b) 3%, (c) 6%, (d) 12% w/w Na_2CO_3 and curing time C= {7, 14, 21, 30} days for the dry methodology.

with minimal amounts of soda ash is a rather slow procedure.

The same applies to Fig. 4 for the wet activation methodology. Each curve represents a different curing time and for completeness, the non-activated dispersion (raw) was included. The results presented in Fig. 4a-d correspond to conditions of pressure 1 atm, and temperature 25 ^{0}C (room temperature).

As in the dry activation methodology, the results from the wet method present linear behavior for shear rates higher than θ_{300} and nonlinear for lower shear rates between θ_3 - θ_{200} fitting quite well on the Herschel-Bulkley model. The results suggest that the optimum curing time is around *14 days* with a *soda ash concentration of 3% w/v* which is the same with the dry activation method. Longer curing times (21 and 30 days) negatively affect the rheological parameters (plastic viscosity and yield stress) but larger quantities of soda ash appear to have a

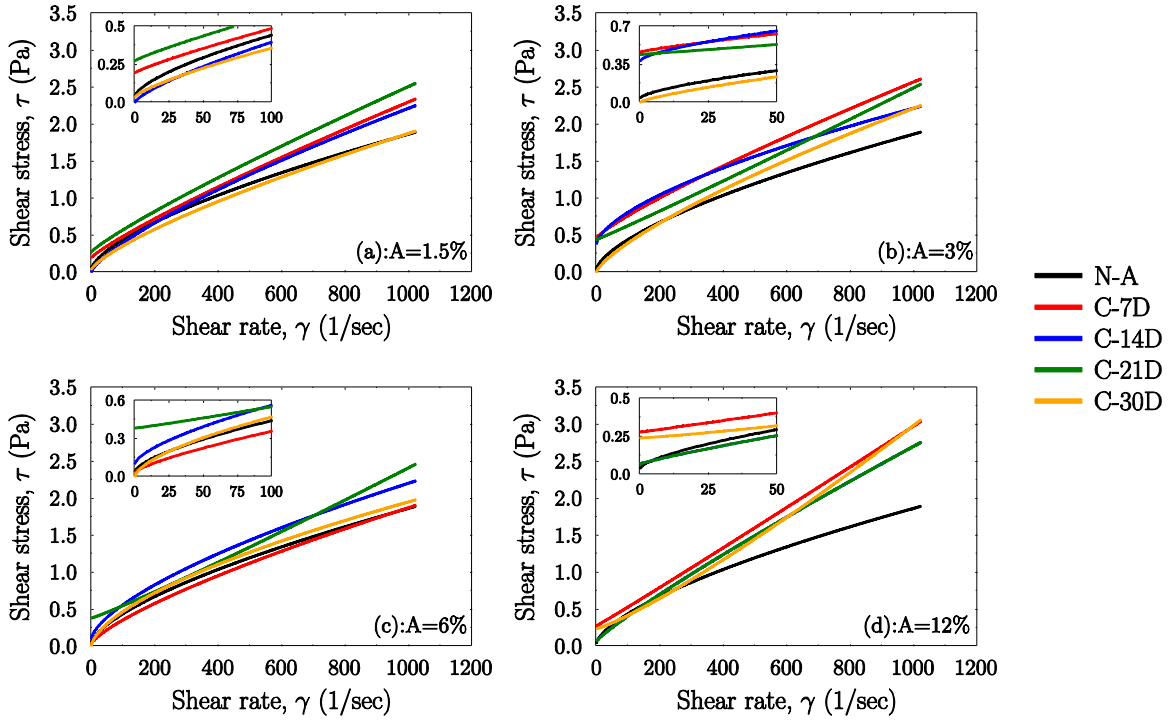

Fig. 4. Rheological curves for various activation concentrations: (a) 1.5%, (b) 3%, (c) 6%, (d) 12% w/v Na_2CO_3 and curing time C= {7, 14, 21, 30} days for the wet methodology.

negative effect. However, the quantity of soda ash corresponding to 1.5% w/v requires more curing time – 21 days to present optimum results denoting that activation is also a slow procedure with the wet methodology.

Fig. 5a to d shows the results from the thermal activation. With this method two different temperature levels, 50 ^{0}C and 80 ^{0}C, and two different agitating times, 16 and 32 h were considered. With these experimental conditions, the chemical reaction speed increases rapidly. It is known that the activation energy doubles every 30 ^{0}C temperature increase, speeding up in this way the chemical reaction of cation exchange. For investigating this effect as a function of agitating time in the cation exchange process, two stirring times were considered by doubling each time. The motivation behind rolling was the agitating procedure that takes place in drilling fluid plants. It is also worth noting that thermal activation can only be applied under wet conditions. The experimental pressure condition in these experiments was 1 atm as under these temperatures no evaporation for the liquid phase was expected.

From Fig. 5, it is observed that by increasing the temperature conditions from 25 ^{0}C (wet method) to 50 ^{0}C and then 80 ^{0}C (wet-thermal method) faster activation is obtained by increasing the chemical reaction activation energy. In this way, the soda ash concentration of 1.5% w/v presents the optimum results when the activation conditions are 50 ^{0}C and 80 ^{0}C, with respect to the rheological behavior. Keeping the temperature constant at 50 ^{0}C but doubling the stirring time from 16 h to 32 h, the 3% w/v soda ash concentration behaves similarly to the experiment containing 1.5% w/v soda ash concentration. It appears that an upper bound of activation has been found. The concentrations (6–12% w/v) do not appear to have a significant impact on rheology. When the temperature is further increased to 80 ^{0}C similar results are observed. More soda ash appears to participate in the activation of bentonite. Finally, by increasing the stirring time to 32 h, the optimum soda ash participating in the activation is raised to 6% w/v. In all methods examined (dry, wet, and thermal) for activating bentonite, the rheological parameters are always higher than the non-activated case.

Having in mind that the API specification requires the shear stress to reach 15.31 Pa when the Couette viscometer operates at 600 rpm [9], we perform a comparison between the optimum bentonite dispersions produced with the different activation methods. The results with the dry and wet activation methods deviate about 6 times from API specification while thermal activation deviates 5 times. To further investigate these results, we have performed XRD analysis for all activation methods tested. However, the results were very similar between the three activation methods, and we chose to present the results for the dry activation only as depicted in Fig. 6. In the diffractogram, we focused on the angles between 3–18° and intensity up to 4000 counts per second (CPS) which is the anticipated area of montmorillonite crystal [37].

The peak that appears at 2θ between the angles 5°∼8° is characteristic of smectite clay minerals. However, bentonite from Polycanthos contains both montmorillonite and beidellite. With increasing the soda ash concentration to investigate the activation efficiency, the peak observed at the angle 2θ increases within the range of 5°∼8°. According to Bragg's law, the d-spacing in the clay minerals is inversely related to the 2θ angles. The observed peak shift suggests that the interlayer space within this range collapses, instead of expanding, due to the increased soda ash concentration. In the natural smectite clay mineral and especially in montmorillonite, Na^+ cations replace exclusively the minor quantities (stemming from the diffractogram) of the Ca^{2+} and Mg^{2+} cations. However, since the montmorillonite is K^+-rich the cation exchange does not improve as expected with soda ash addition and instead the basal spacing of the natural smectite to decrease, vaguely, it increases within the angles 5°∼8°. This result is attributed to the so-called *illite-smectite transformation phenomenon* which predominates resulting in poor activation of the natural smectite clay mineral. It is well-known that the peak that appears near 2θ∼12° in the XRD spectrum of the raw material is characteristic of the illite/mica clay mineral and many times is K^+ rich.

According to [37], the *transformation phenomenon* is responsible for the formation of *beidellite* clay mineral. Furthermore, the essential conditions for transforming illite to smectite-like clay mineral are satisfied (i.e. *de-potassificaton, de-alumination,* and *silication*) by reducing the layer charge so that the K^+ are released from the interlayer space of illite at

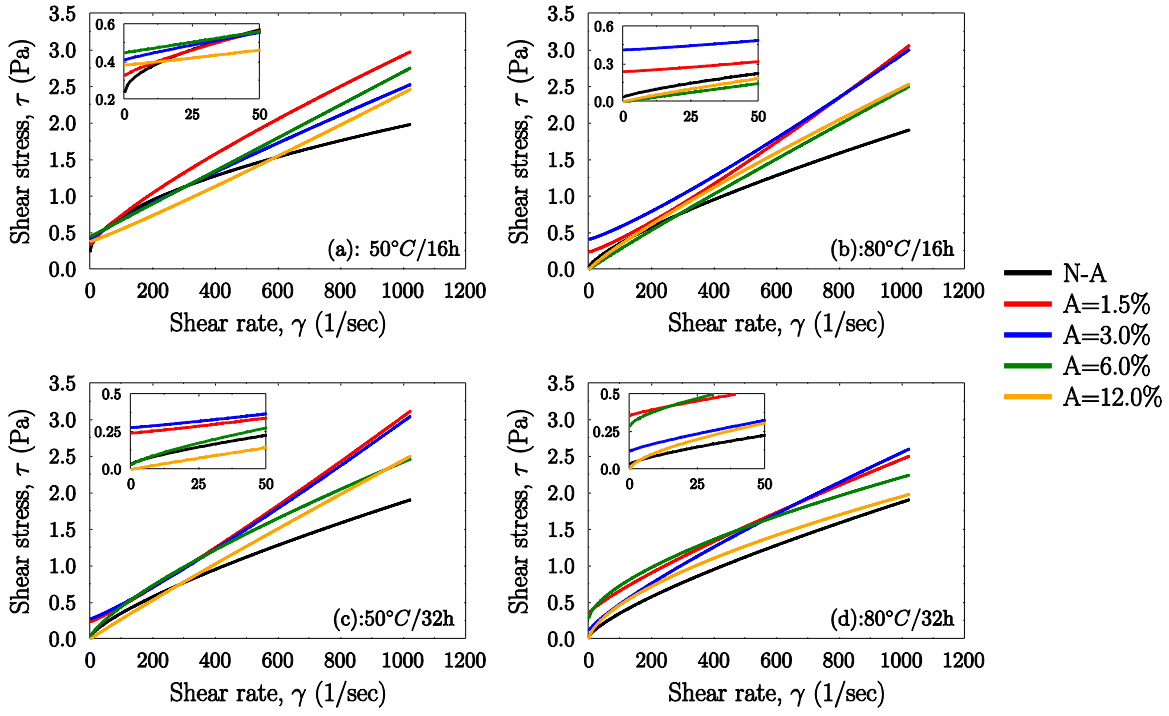

Fig. 5. Rheological curves for various activation concentrations, temperature level, and stirring time for the thermal activation methodology. ***(a)*** 50 ^{0}C/16 h, ***(b)*** 80 ^{0}C/16 h, ***(c)*** 50 ^{0}C/32 h, and ***(d)*** 80 ^{0}C/32 h.

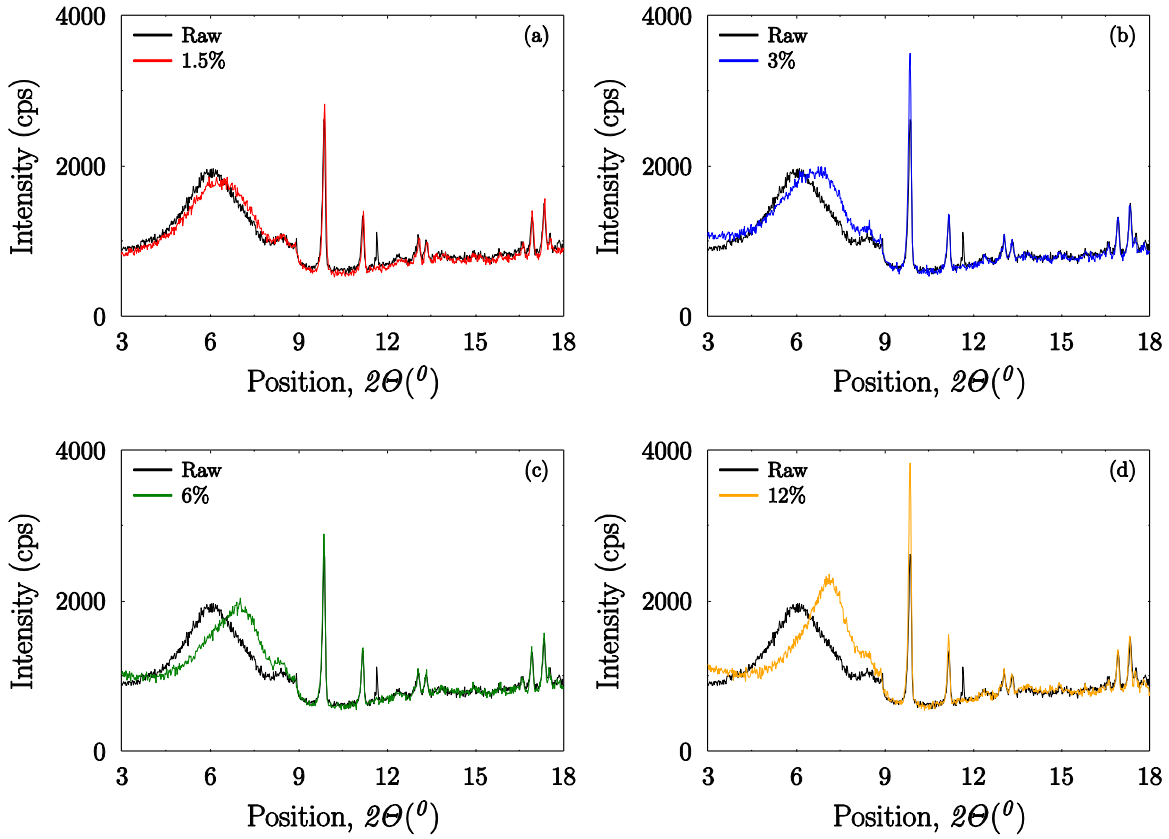

Fig. 6. Comparison of XRD spectrum of the < 2 μm fraction between raw Polycanthos bentonite and activated with ***(a)*** 1.5% w/w, ***(b)*** 3% w/w, ***(c)*** 6% w/w, and ***(d)*** 12% w/w soda ash.

high pH values (> 7.5). With increasing the soda ash content for better activation, the alkalic environment prevails, the protons concentration decreases causing the pH to increase thereby amplifying the transformation phenomenon. Moreover, because of the exchange of the cation species from the natural smectite clay minerals, the released Ca^{2+} and Mg^{2+} (an essential condition of the transformation) are responsible for the K^{+} dislodgement from the illite clay mineral. For the extreme case of 12% w/w soda ash, illite is most probably that it has been completely transformed to beidellite. Other similar works done in the same deposit report that Polycanthos bentonite mineral assemblage includes smectites as major and illite/mica as minor minerals supporting the low intensity of the peak [7].

Our hypothesis that illite has completely transformed to beidellite at high soda ash content (12% w/w), is supported by the fact that the peak in the diffractogram that is representative of raw illite peak vanishes after the activation attempt. At the same time the peak that is representative of the natural smectite becomes more intense (~2500 CPS) and shifts from low to slightly higher 2θ angles, indicating low d-spacing in smectite clay minerals due to the transformation phenomenon. Even though, beidellite is a smectite clay mineral the interlayer cations in its structure are held more tightly and do not easily exchange for the desired Na^{+} activation while at the same time the other smectitic clay minerals that are K^{+}-rich in Polycanthos deposit act as an inhibitor to the complete cation exchange.

For completeness in the following part of the analysis we present the outcomes of the rheological results in the form of bar charts. Figs. 7a to 7f presents the plastic viscosity (vertical left column) and yield point (vertical right column) of the produced dispersions that were created with the different activation methods. Each group of bars (4 in total) corresponds to different activation days for the dry and wet methods while the thermal method represents conditions. Each bar corresponds to the activation percentage.

It is shown that plastic viscosity and yield point practically present similar behavior for the dry activation method and are constant for the soda ash concentration and activation time. On the other hand, plastic viscosity and yield point present an increasing trend with curing time and soda ash concentration up to 3% w/v for the wet activation method. Finally, with thermal activation, the plastic viscosity appears to improve for all cases examined but the yield point in most cases becomes negligible. This might be attributed to the heat and stirring time. It is seen that 50 ^{0}C temperature and 16 h stirring time yields the optimum results.

Fig. 8a to f shows the 10 s (vertical left column) and 10 min (vertical right column) gel strength for all activation methods. Results from this Figure suggest that with the dry activation method, the 10 s gel strength increases with both soda ash concentration and curing time. The 10 min gel strength presents a similar behavior. When examining the wet activation method, the 10 s and the 10 min gel strength presents optimum results for curing time between 14 and 21 days and for soda ash concentrations between 1.5–3% w/v. Finally, with the thermal activation method, the 10 s gel strength presents similar behavior for the two different temperatures (50 ^{0}C-80 ^{0}C) and stirring times (16 h-32 h). For the 10 min gel strength, the optimum results are obtained with 50 ^{0}C temperature and 16 h stirring time.

4.2. *Activations' performance: filtration properties*

To obtain a complete understanding of the activation methods, the filtration properties with low-pressure and low-temperature LPLT filter press were also studied. Fig. 9 presents the results from the LPLT for all the activation methods examined. Results are reported as the 30-minute filtrate loss (vertical left column) and the cake thickness in mm (right left column) that is built up on the filter during experimentation. Each group of bars corresponds to different activation days for the dry and

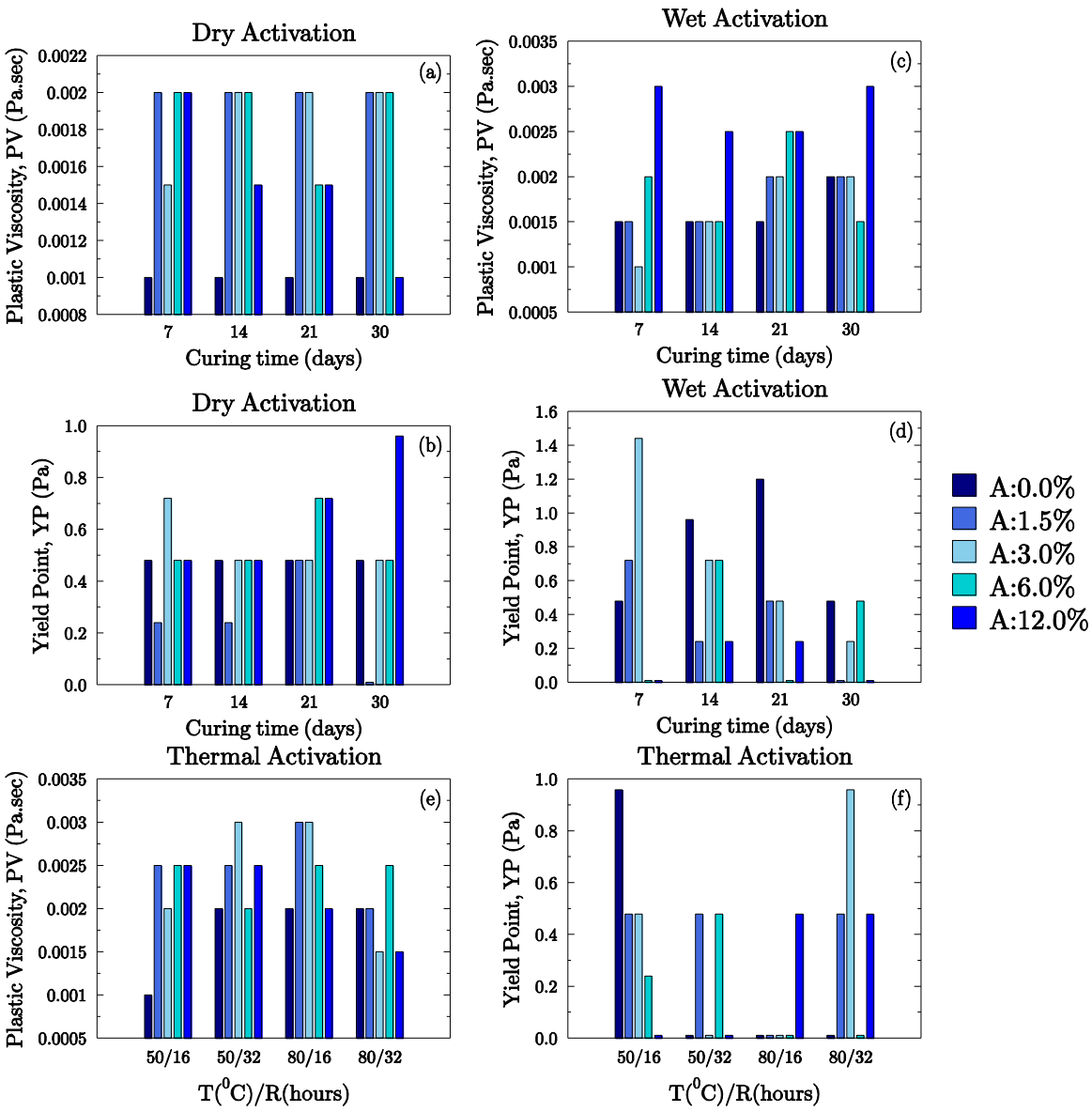

Fig. 7. Plastic viscosity and yield point of the activation methods.

wet methods while the thermal method represents conditions. Each bar corresponds to the activation percentage.

From the results presented in Fig. 9, it is seen that the filtrate loss, for the dry activation method, is minimum when the soda ash concentration is 1.5% w/w and for all curing days. As expected, the respective cake thickness is the lowest compared with the other cases. The worse filtration losses and cake thickness occur when the soda ash concentration is higher than 3% w/w. The wet activation method yields the lowest filtrate loss and cake thickness when the soda ash concentration is 1.5% w/v. Interestingly, the non-activated bentonite shows even lower values suggesting that the wet activation is an effective method used by the industry. Curing time appears to have minimal effect with the wet activation method on filtration results. Finally, with the thermal activation method, the most effective filtrate loss and cake thickness are obtained when the conditions are 50 ^{0}C temperature and 16 h stirring time. Filtration parameters change significantly with temperature and stirring time. Comparing the results with the suggested values from API [9] requiring that the filtrate loss must be $>$ 15 mL we see that the bentonite dispersions do not qualify according to API specifications. As explained earlier this is due to the presence of the K^{+} which acts negatively on the swelling characteristics of the dispersion but also its filtration properties. This is also consistent with the analysis presented in [7].

4.3. Performance of Polymer amended drilling fluid systems

Based on the activation performance results obtained we consider that bentonite clay could be further amended with polymers to enhance its properties and qualify according to API standards as low density solid in drilling fluid systems.

In the industry, several polymers are available for enhancing and improving bentonite swelling capacity after activation. Polymers include within their structure ionizable functional groups and when exposed to water they ionize into cations or anions. This is the reason why they present hydrophilic behavior and when in contact with fresh or salt water enhance the drilling fluid with respect to its filtration properties but also to its rheological behavior, enhancing its viscosity. The different types of polymers can modify bentonite either by changing or by upgrading the clay mineral layer surface charge of the clay mineral layers, so more water is able to enter the interlayer space, hence increasing substantially the swelling ability. Polymer-amended bentonite can be cationic, anionic, or non-ionic. Xanthan gum is an

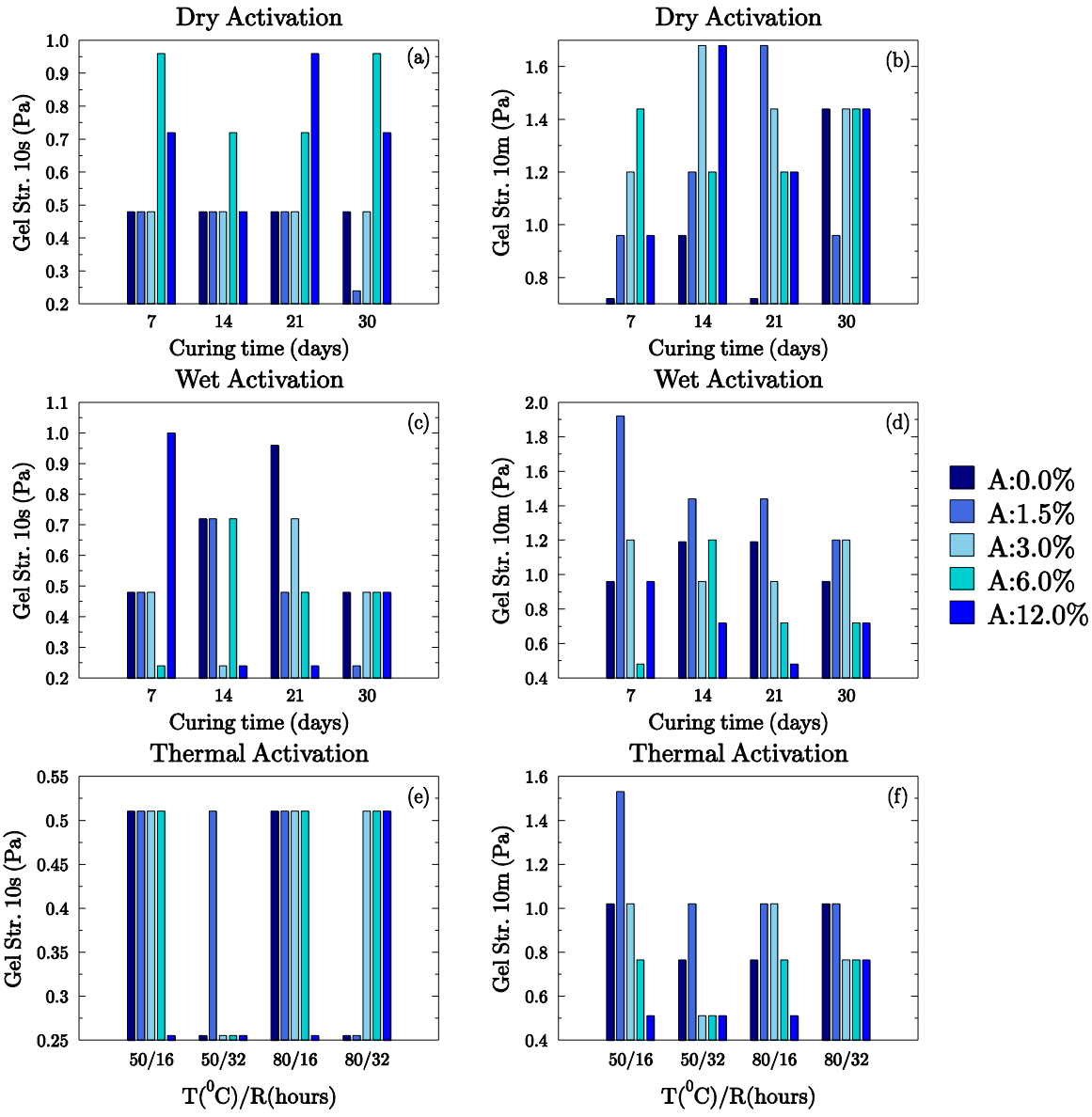

Fig. 8. Gel strength of the activation methods.

anionic polymer, and this kind is preferred over the other two because it creates more stable and efficient colloids because of the development of multiple species of bonds and interactions with bentonite. This category of polymer consists of the functional group -COOH that deprotonates and becomes negatively charged -COO^- when mixed with water. As a result, the montmorillonite clay mineral layer charge is influenced by the carboxylate anion group because it contributes to the mechanism of colloid creation by creating (i) hydrogen bonding, (ii) electrostatic attraction, and (iii) cation bridging adsorption [29].

Fig. 10a to d presents the rheological curves of the drilling fluid systems that were prepared to simulate the upper (DFS-1) and lower (DFS-2) well sections. The required additives and quantities used in the experiments are summarized in Tables 1–4. Each drilling fluid system corresponding to the upper and lower well section was prepared with commercial bentonite and with the thermally activated bentonite from Polycanthos quarry creating four groups of experiments. Each curve corresponds to different xanthan gum mass added in the system, ranging from 0 gr (no xanthan gum added) to 4 gr. For comparisons, we have included the API requirement of 15.31 Pa at 600 rpm (annotated as API on the Figures-black dot). The drilling fluid systems were prepared after thermally activating Polycanthos bentonite, and then all the other additives were mixed to compose the final systems. For the commercial, immediate mixing with the additives was performed. Standard experimental conditions were considered, P = 1 atm and T = 25 ^{0}C.

From Fig. 10a we observe that the rheological curve with commercial bentonite without the addition of xanthan gum (0-X.gum) qualifies according to the API standard. From that point, any addition of polymer further enhances the DFS. It is worth noting that DFS without xanthan gum obeys the Bingham plastic rheological model while with addition of polymer obeys the Hershel-Bulkley. On the other hand, Fig. 10b shows that with the addition of >1 gr xanthan gum thermally activated bentonite clay qualifies according to API and with more mass of polymer further enhances its properties. This rheological behavior is better described by the Herschel-Bulkley model. From the results presented in Fig. 10c, we observe that for the lower well section where 6 gr of bentonite is used (see Table 3), polymer upgrade is also required at quantities of more than 1 gr. This is explained by the fact that for the upper well section 22.5 gr of commercial bentonite is used while in the lower well section, the commercial bentonite quantity added is significantly lower (3.75 times lower) thus requiring enhancement to satisfy

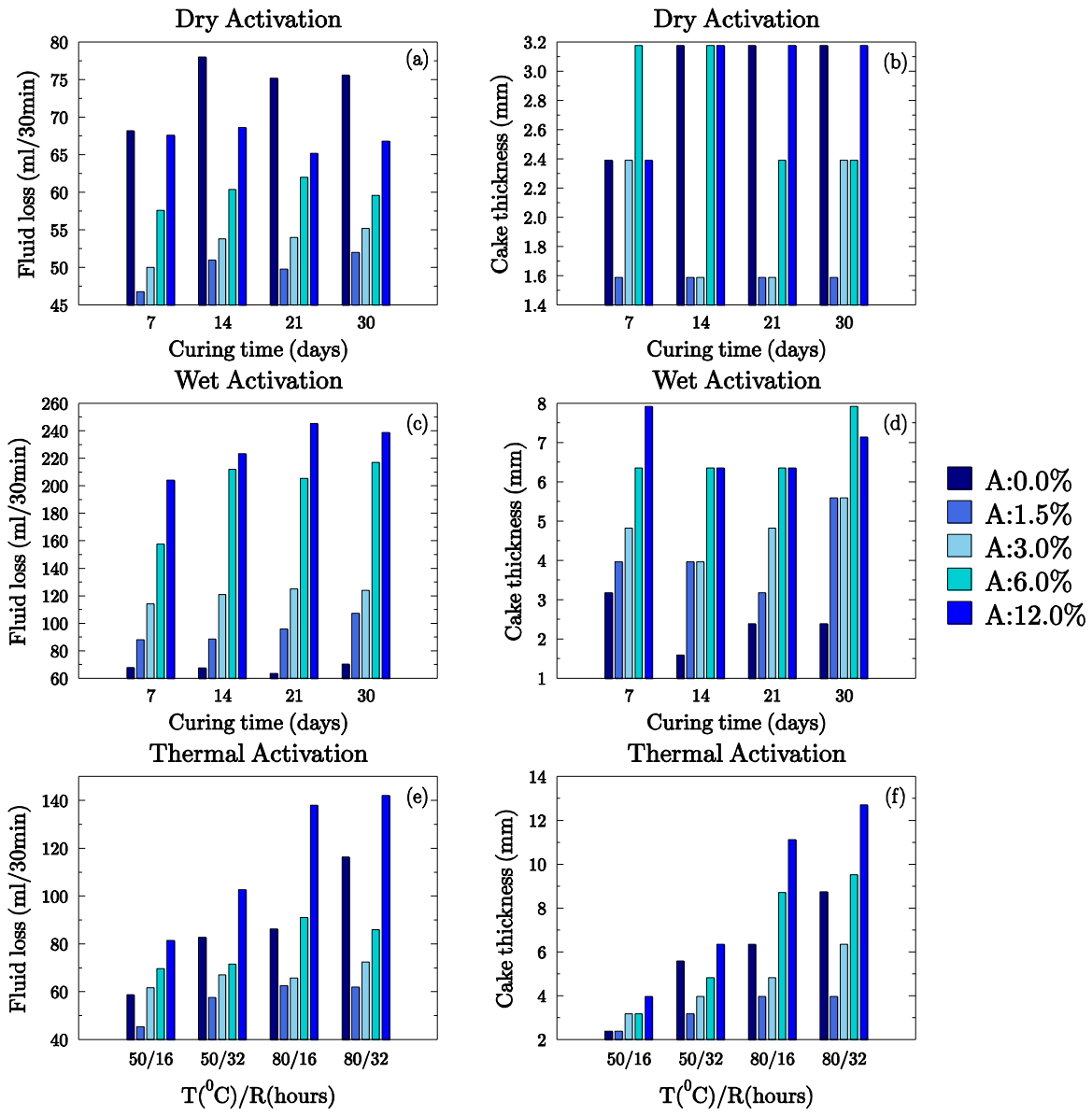

Fig. 9. Filtration control (filtrate losses and cake thickness) for all activation methods.

API. Finally, Fig. 10d shows that for the lower well section, a quantity of ~1.5 gr of xanthan gum is required to satisfy API. Any larger quantities of polymer just further enhance its performance. The reason why the lower well section with thermally activated bentonite requires more polymer mass is due to the presence of KOH and NaOH cause the pH to increase substantially, and the mixture becomes highly alkaline which affects the function of the polymer and increases viscosity, thus creating a better colloid [30,31].

Fig. 11 presents the plastic viscosity (11a & 11c) and yield point (11b & 11d) parameters of the drilling fluid systems created with commercial and thermally activated bentonite respectively. In both drilling fluid systems (DFS-1) and (DFS-2), the plastic viscosity PV, and yield point YP, values increase with the addition of the polymer mass. Also, another observation is that the plastic viscosity values with thermally activated bentonite in DFS-1 present somewhat lower values compared to the DFS-1 with commercial bentonite. However, the yield point obtained with thermally activated compares quite well with the commercial if more mass of xanthan gum is used at a ratio of 1:2. Interestingly, the plastic viscosity and yield point values with thermally activated bentonite in DFS-2 approach the values of DFS-2 with commercial bentonite. This is attributed to the low quantity of bentonite (6 gr) that was used to simulate the lower well section suggesting that the polymer dominates in the generated parameters of PV and YP. This ascertainment can be attributed to the fact that when the polymer additive is mixed with bentonite clay PV and YP values increase as expected because more carboxylate groups are ionized in xanthan gum and develop more cation bridging adsorption, hydrogen bonding, and electrostatic attraction between the negatively charged – COO^-, and cations of interlayer space to enhance its properties to meet API specification thus forming a more gelled/colloidal structure [11,29].

Fig. 12 represents the results obtained for the 10 s and 10 min gel strength of the drilling fluid systems for the upper and lower well sections. The 10 s gel strength of DFS-1 with both commercial and thermally activated bentonite tends to present thixotropic behavior with xanthan gum mass addition. The values range between 15–20 Pa for the DFS-1 with commercial and 5–20 Pa for the DFS-1 with thermally activated bentonite. This observation shows a 5 Pa increase with xanthan gum addition in the DFS-1 with commercial bentonite while a 15 Pa increase in the DFS-1 with the thermally activated bentonite. Similar behavior is observed for the 10 min gel strength with slightly

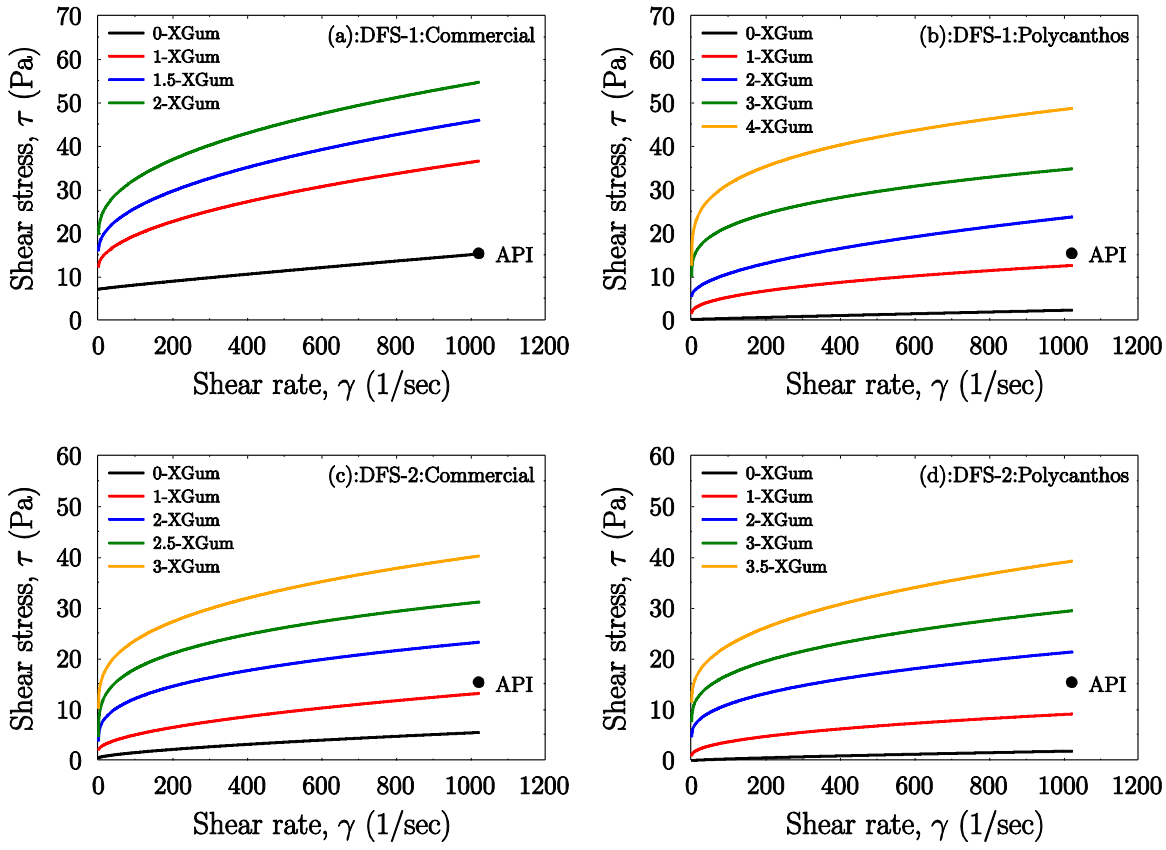

Fig. 10. Rheological curves of the drilling fluid systems (DFS-1: upper well section 10a & 10b) and (DFS-2: lower well section 10c & 10d) with commercial and thermally activated bentonite. (a) DFS-1A commercial, (b) DFS-1B thermally activated, (c) DFS-2A commercial, (d) DFS-2B thermally activated.

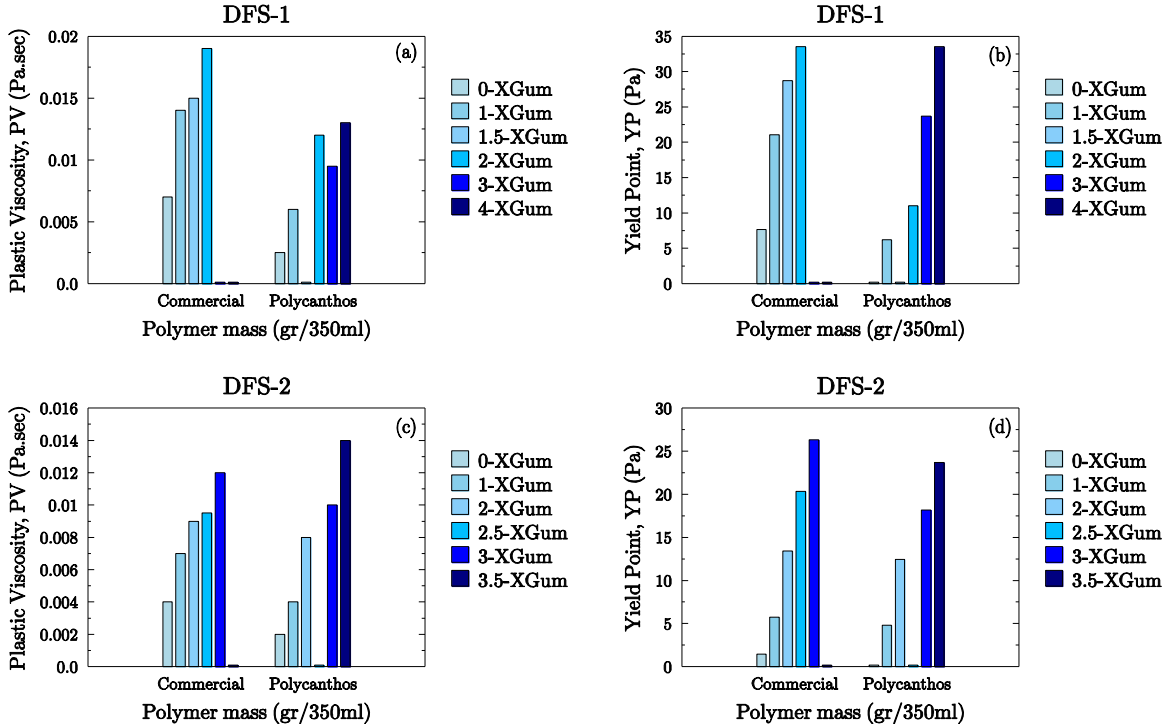

Fig. 11. Plastic viscosity and yield point parameters (DFS-1: upper well section 11a & 11b) and (DFS-2: lower well section 11c & 11d) with commercial and thermally activated bentonite.

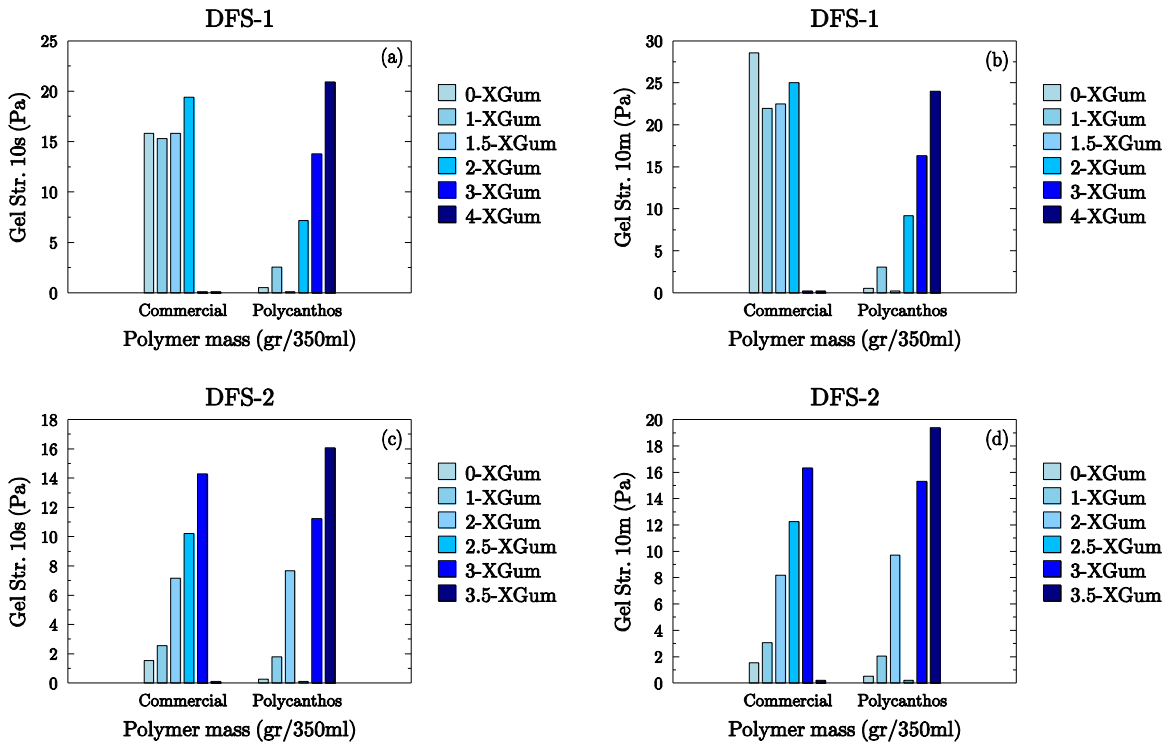

Fig. 12. Gel strength 10 s and 10 m (DFS-1: upper well section 12a & 12b) and (DFS-2: lower well section 12c & 12d) with commercial and thermally activated bentonite.

elevated strength values. For the DFS-2 with commercial and thermally activated bentonite, the range of values is higher for both the 10 s and 10 min gen strength. This can be explained by the strong action of the polymer and the low mass of bentonite clay. This behavior is consistent with the explanation that more carboxylate groups are ionized in xanthan gum and develop more cation bridging adsorption, hydrogen bonding, and electrostatic attraction thereby improving the gel strength performance.

The characterization of colloidal structures that are created after polymer addition at different spatial scales often involves multiple

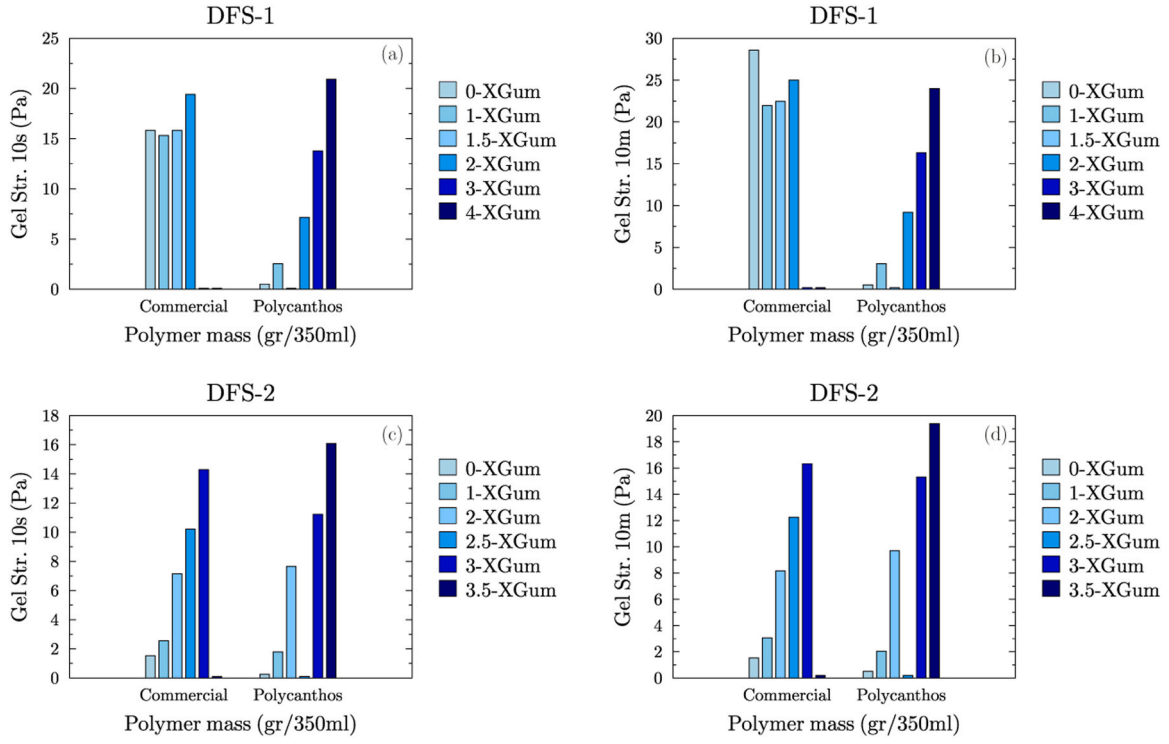

Fig. 13. Filtrate losses and cake thickness (DFS-1: upper well section 13a & 13b) and (DFS-2: lower well section 13c & 13d) with commercial and thermally activated bentonite.

techniques. Then the information obtained from the various tests helps build a comprehensive understanding of the constructed colloidal systems. In practice, the most common technique that is employed for assessing the stability of the colloidal systems is the determination of the zeta potential and surface charge which are highly helpful for optimizing the stability conditions for various applications. If the magnitude and sign (either positive or negative) of the zeta potential is high, then it is an indication of the strength and stability of the colloidal system while at the same time preventing flocculation. Other techniques include scanning electron microscopy (SEM) for examination at mesoscopic and dynamic light scattering (DLS) at the microscopic scale. For colloidal systems used for drilling fluid applications at macroscopic scale, rheology is considered to be adequate for evaluating how the colloidal suspensions respond to applied shear rate providing information about their flow properties (e.g., viscosity and yield point). Then, if the determined values satisfy the API standards, it is a good indicator that the polymer was adsorbed, and the colloidal composite structure was successfully created.

We complete our analysis with a discussion on filtration losses of the two drilling fluid systems considered. Fig. 13 presents the filtrate loss in mL (13a & 13c) and the cake thickness (13b & 13d) for the DFS-1 and DFS-2 respectively. For comparisons, we have included the 15 mL threshold requirement as stipulated by API.

As can be seen from Fig. 13a & c, with the addition of xanthan gum the filtrate losses decrease for both drilling fluid systems (upper and lower well sections) and drop below the 15 mL threshold of API. Consistently, the cake-building thickness is also reduced with polymer mass addition and is associated with filtrate losses. If higher filtration control is required, then higher quantities of xanthan gum mass can be used for the thermally activated bentonite.

To complete the discussion, we present in Fig. 14 representative filter cakes obtained from the upper well section drilling fluid system amended with 1 gr xanthan gum blended with commercial (Fig. 14a) and thermally activated bentonite (Fig. 14b).

5. Conclusions

The contribution of this work lies in its comprehensive approach to repurposing waste bentonite for water-based drilling fluids, addressing environmental concerns, optimizing the activation process, introducing polymer amendments, and ensuring compliance with industry standards. This work showcases a holistic solution with potential implications for both environmental sustainability and economic viability in drilling operations. Specifically, the following conclusions can be summarized:

- The thermal activation method appeared to be more efficient than the dry and wet activation methods. The rheological behavior of all three groups of bentonite dispersions compares quite well with the Hershel-Bulkley model over the entire range of shear rates.
- All activation methods improve the raw material in both rheological and filtration control parameters to an extent, however, not meet the API specifications. Both dry and wet activation methods yielded optimum results with 1.5-3% soda ash concentration and 14-21 curing days. For the thermal activation method, optimum results were obtained with conditions of 50 ^{0}C temperature and 16 h stirring time. Generally, thermal activation appears to work better with respect to rheological parameters and filtration control than the dry and wet activation methods and is time-effective.
- The inability to successfully activate the raw material with the presented three methods is attributed to the K^{+}-rich montmorillonite and beidellite clay mineral contained in bentonite which renders its conversion to Na-bentonite a challenge. Due to the high layer charge in montmorillonite clay mineral, its interlayer space collapses making montmorillonite selective for K^{+} cations thereby preventing hydration. Also, beidellite clay mineral that was formed from the illite-smectite transformation phenomenon possibly contributes to the inability of full bentonite activation. Although, the activation of the material is successful to an extent, might be due to the exchange of Ca^{2+} and Mg^{2+} with Na^{+} in the interlayer space of natural smectite clay minerals. As such, the presence of K^{+} in montmorillonite and beidellite clay minerals inhibit complete activation of the material, even though the latter is a member of the smectite group which exhibit excellent swelling behavior, beidellite is a special case that does not swell to the desired degree.
- The drilling fluid systems for the upper and lower well sections that were experimentally tested showed significant improvement after amending bentonite clay with xanthan gum polymer. With the addition of xanthan gum polymer mass of about 1-1.5 gr, both drilling fluid systems satisfy the viscosity ($\tau > 15.31$ Pa) and filtration control (< 15 mL) of API.

The results from this work show that either by amending or enhancing local clays could be potentially used as additives in drilling fluids leading to the development and sustainability of local resources.

CRediT authorship contribution statement

Sarris Ernestos: Conceptualization, Formal analysis, Investigation, Methodology, Project administration, Resources, Supervision, Validation, Visualization, Writing – original draft, Writing – review & editing.

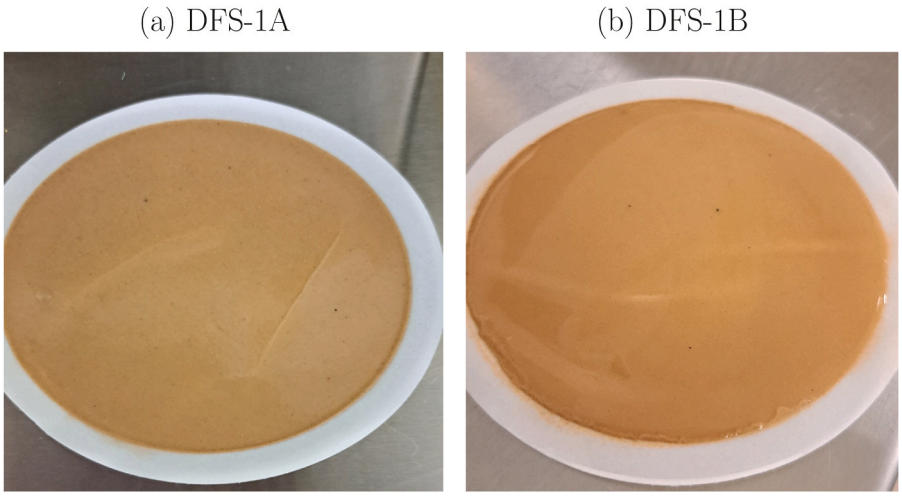

Fig. 14. Filter cakes obtained with (a) commercial bentonite (DFS-1A) and (b) with thermally activated bentonite (DFS-1B) amended with 1 gr X.gum.

Gravanis Elias: Conceptualization, Formal analysis, Supervision, Writing – review & editing. **Ramsis Youstina:** Conceptualization, Formal analysis, Investigation, Methodology, Validation, Writing – original draft, Writing – review & editing, Data curation.

Declaration of Competing Interest

The authors declare that they have no known competing financial interests or personal relationships that could have appeared to influence the work reported in this paper.

Data availability

No data was used for the research described in the article.

Acknowledgments

The successful completion of this research would not have been possible without the support and collaboration from Hellenic Mining Company Ltd. We extend our sincere appreciation to Mr Demetris Vattis, Mining Director for his valuable contribution in providing the essential raw materials crucial to our study and constructive discussions.

References

[1] P. Lee, E. Sims, O. Bertham, H. Symington, N. Bell, L. Pfaltzgraff, P. Sjögren, H. Wilts, M. O'Brien, Towards a circular economy: waste management in the EU; study, Eur. Union (2017), https://doi.org/10.2861/978568.
[2] M. Regueiro, A. Alonso-Jimenez, Minerals in the future of Europe, Miner. Econ. 34 (2021) 209–224, https://doi.org/10.1007/s13563-021-00254-7.
[3] D. Shiquan, X. Deyi, Z. Yonguang, R. Keenan, Critical mineral sustainable supply: Challenges and governance, Futures 146 (2023), 103101, https://doi.org/10.1016/j.futures.2023.103101.
[4] E. Gravanis, E. Sarris, A working model for estimating CO_2-induced uplift of cap rocks under different flow regimes in CO_2 sequestration, Geomech. Energy Environ. (2023), 100433, https://doi.org/10.1016/j.gete.2023.100433.
[5] R.M. Johannsen, B.V. Mathiesen, K. Kermeli, W. Crijns-Graus, P.A. Østergaard, Exploring pathways to 100% renewable energy in European industry, Energy 268 (2023), 126687, https://doi.org/10.1016/j.energy.2023.126687.
[6] Y. Ramsis, E. Sarris, L. Papaloizou, E. Gravanis, D. Vattis, The influence of activation methodologies on the rheological and filtration characteristics of Cyprus smectites for potential use as low density solids in drilling fluids. A case study of Polycanthos quarry, in: American Rock Mechanics Association (ARMA), Atlanta, Georgia - USA, 2023.
[7] G.E. Christidis, Genesis and compositional heterogeneity of smectites. Part III: Alteration of basic pyroclastic rocks - A case study from the Troodos Ophiolite Complex, Cyprus, Mineral. Soc. Am. (2006), https://doi.org/10.2138/am.2006.2001.
[8] API 13A: Drilling Fluids Materials, American Petroleum Institute, 2020. ⟨https://global.ihs.com/doc_detail.cfm?document_name=API%20SPEC%2013A&item_s_key=00010450⟩ (accessed August 9, 2022).
[9] API 13B-1: Field Testing Water-based Drilling Fluids, American Petroleum Institute, 2021. ⟨https://www.bsbedge.com/productdetails/API/APIRP13B-1/api rp13b-1⟩ (accessed June 5, 2023).
[10] F. Uddin, Introductory Chapter: Montmorillonite Clay Consumption Trend in Industry. Montmorillonite Clay, IntechOpen,, 2021, https://doi.org/10.5772/intechopen.101362.
[11] P.F. Luckham, S. Rossi, The colloidal and rheological properties of bentonite suspensions, Adv. Colloid Interface Sci. 82 (1999) 43–92. ⟨www.elsevier.nl/locate/cis⟩ (accessed June 5, 2023).
[12] F. Bergaya, G. Lagaly, General introduction: clays, clay minerals, and clay science. Developments in Clay Science, Elsevier,, 2006.
[13] I.E. Odom, Smectite clay minerals: properties and uses, Math. Phys. Sci. (1984) 391–409, https://doi.org/10.1098/rsta.1984.0036.
[14] B. Ndlovu, E. Forbes, S. Farrokhpay, M. Becker, D. Bradshaw, D. Deglon, J. Kruttschnitt, A preliminary rheological classification of phyllosilicate group minerals, Min. Eng. 55 (2013) 190–200, https://doi.org/10.1016/j.mineng.2013.06.004.
[15] G.E. Christidis, Mechanism of illitization of bentonites in the geothermal field of Milos Island Greece: Evidence based on mineralogy, chemistry, particle thickness and morphology, Clays Clay Min. 43 (1995) 569–585, https://doi.org/10.1346/CCMN.1995.0430507.
[16] L. Ohazuruike, K.J. Lee, A comprehensive review on clay swelling and illitization of smectite in natural subsurface formations and engineered barrier systems, Nucl. Eng. Technol. 55 (2023) 1495–1506, https://doi.org/10.1016/j.net.2023.01.007.
[17] M.S. Hassan, N.A. Abdel-Khalek, Beneficiation and applications of an Egyptian bentonite, Appl. Clay Sci. 13 (1998) 99–115, https://doi.org/10.1016/S0169-1317(98)00021-0.
[18] S. Boussen, D. Sghaier, F. Chaabani, B. Jamoussi, S.Ben Messaoud, A. Bennour, The rheological, mineralogical and chemical characteristic of the original and the Na2CO3-activated Tunisian swelling clay (Aleg Formation) and their utilization as drilling mud, Appl. Clay Sci. 118 (2015) 344–353, https://doi.org/10.1016/j.clay.2015.10.017.
[19] K. Bahranowski, A. Klimek, A. Gaweł, E.M. Serwicka, Rehydration Driven Na-Activation of Bentonite—Evolution of the Clay Structure and Composition, Materials Vol. 14 (2021) 7622, https://doi.org/10.3390/ma14247622.
[20] M. Magzoub, M. Mahmoud, M. Nasser, I. Hussein, S. Elkatatny, A. Sultan, Thermochemical Upgrading of Calcium Bentonite for Drilling Fluid Applications, J. Energy Resour. Technol. 141 (2019), https://doi.org/10.1115/1.4041843.
[21] M.I. Magzoub, M.S. Nasser, I.A. Hussein, A. Benamor, S.A. Onaizi, A.S. Sultan, M. A. Mahmoud, Effects of sodium carbonate addition, heat and agitation on swelling and rheological behavior of Ca-bentonite colloidal dispersions, Appl. Clay Sci. 147 (2017) 176–183, https://doi.org/10.1016/j.clay.2017.07.032.
[22] C. Karagüzel, T. Çetinel, F. Boylu, K. Çinku, M.S. Çelik, Activation of (Na, Ca)-bentonites with soda and MgO and their utilization as drilling mud, Appl. Clay Sci. 48 (2010) 398–404, https://doi.org/10.1016/j.clay.2010.01.013.
[23] F. Boylu, Modelling and optimisation of ageing characteristics of soda activated Na +-bentonites, Appl. Clay Sci. 83–84 (2013) 300–307, https://doi.org/10.1016/j.clay.2013.08.024.
[24] G.E. Christidis, Industrial Clays, in: European Mineralogical Union Notes in Mineralogy, Universitat Jena - Mineralogie, 2011, pp. 341–414, https://doi.org/10.1180/EMU-NOTES.9.9.
[25] B. Toka, Use of borates as an activating agent for drilling mud bentonites, 2008. ⟨https://open.metu.edu.tr/handle/11511/17618⟩ (accessed June 9, 2022).
[26] M. Mahmoud, A. Mohamed, M.S. Kamal, A. Sultan, I. Hussein, Upgrading Calcium Bentonite to Sodium Bentonite Using Seawater and Soda Ash, Energy Fuels 33 (2019) 10888–10894, https://doi.org/10.1021/acs.energyfuels.9b02900.
[27] G.F. Al-Ghanimi, N.S. Al-Zubaidi, The Performance of Iraqi Bentonite Using Soda Ash and Caustic Soda Additives, Assoc. Arab Univ. J. Eng. Sci. 27 (2020) 83–93, https://doi.org/10.33261/jaaru.2019.27.1.010.
[28] B.E. Şans, O. Güven, F. Esenli, M.S. Çelik, Contribution of cations and layer charges in the smectite structure on zeta potential of Ca-bentonites, Appl. Clay Sci. 143 (2017) 415–421, https://doi.org/10.1016/j.clay.2017.04.016.
[29] Q. Cui, B. Chen, Review of polymer-amended bentonite: Categories, mechanism, modification processes and application in barriers for isolating contaminants, Appl. Clay Sci. 235 (2023), 106869, https://doi.org/10.1016/j.clay.2023.106869.
[30] D.F.S. Petri, Xanthan gum: A versatile biopolymer for biomedical and technological applications, J. Appl. Polym. Sci. 132 (2015) 42035, https://doi.org/10.1002/app.42035.
[31] J. Patel, B. Maji, N.S.H.N. Moorthy, S. Maiti, Xanthan gum derivatives: review of synthesis, properties and diverse applications, RSC Adv. 10 (2020) 27103–27136, https://doi.org/10.1039/D0RA04366D.
[32] C. Apostolidou, E. Sarris, A. Georgakopoulos, Dynamic thermal aging of water-based drilling fluids with different types of low-rank coals as environmental friendly shear thinning additives, J. Pet. Sci. Eng. 208 (2022), 109758, https://doi.org/10.1016/j.petrol.2021.109758.
[33] V.C. Kelessidis, R. Maglione, Modeling rheological behavior of bentonite suspensions as Casson and Robertson–Stiff fluids using Newtonian and true shear rates in Couette viscometry, Powder Technol. 168 (2006) 134–147, https://doi.org/10.1016/j.powtec.2006.07.011.
[34] V. Kelessidis, R. Maglione, Yield stress of water-bentonite dispersions, Physicochem. Eng. Asp. 318 (2008) 217–226, https://doi.org/10.1016/j.colsurfa.2007.12.050.
[35] J.S. Arora. Introduction to Optimum Design, Fourth edition.,, Elsevier,, 2017, https://doi.org/10.1016/C2013-0-15344-5.
[36] R. Caenn, H.C.H. Darley, G.R. Gray. Composition and Properties of Drilling and Completion Fluids, Seventh edition.,, Elsevier Inc,, 2016. ⟨http://www.sciencedirect.com:5070/book/9780128047514/composition-and-properties-of-drilling-and-completion-fluids⟩. accessed January 30, 2023.
[37] M.E. Essington, Soil and Water Chemistry: An Integrative Approach, CRC Press,, 2003, https://doi.org/10.1201/B12397.